

The Velocity Correlation Function for the Lorentz Gas

R. G. Cole^{1,2} and T. Keyes¹

Received August 15, 1984; revision received December 11, 1987

The results of variational solutions of the repeated ring and self-consistent repeated ring equations for the two- and three-dimensional overlapping Lorentz gas (LG), as formulated in a previous report, are presented. Calculations of the full velocity correlation function (VCF) for the 2D LG, including long-time tails, are compared with those from molecular dynamics. The trial functions chosen lead to predictions for the long-time tails that improve as the density of the scatterers is increased. At a value of 0.24 for ρ^* ($=\rho\sigma^2$, where ρ is the density and σ the radius of scatterers), the self-consistent amplitudes of the long-time tail are within 40% of the molecular dynamics. A limited number of 3D results for the short-time behavior of the repeated ring VCF are presented. The 3D solutions agree with the molecular dynamics to within 10%.

KEY WORDS: Kinetic theory; random media; Lorentz model; self-consistent repeated ring theory; long-time tails.

1. INTRODUCTION

The Lorentz model has received considerable attention because it represents one of the simplest nontrivial models of particle transport through random media. The Lorentz model we consider (the overlapping Lorentz gas, LG) consists of a random array of fixed overlapping scatterers of radius σ , through which a tagged point particle travels. When the density ρ^* of the fixed scatterers is low ($\rho^* = \rho\sigma^d \ll 1$, where d is the dimension of the system), the motion of the tagged particle is described by the Lorentz-Boltzmann equation. Here, tagged-particle-scatterer-correlations are ignored. As the density is increased, the correlations become important and a more sophisticated theory is required, the repeated ring (RR)

¹ Department of Chemistry, Boston University, Boston, Massachusetts 02215.

² Present address: AT&T Bell Laboratories, Holmdel, New Jersey 07733.

theory.⁽²⁾ The repeated ring equations incorporate pair correlations and represent an improvement over the Boltzmann equation at moderate densities. Yet, as the tagged particle explores more and more of the matrix of scatterers, still higher order correlations develop. These higher order correlations play a prominent role as the density increases, and, indeed, lead to the vanishing of the particle's diffusion constant D at the percolation density ρ_c^* .⁽³⁾ The repeated ring equations fail to predict the vanishing D , but a self-consistent theory,^(1,4-7) incorporating these higher order correlations (rings inside of ring collisions⁽⁴⁾), does predict well the vanishing of D .

The fundamental quantity reflecting all the important physics discussed in the preceding paragraph is the velocity correlation function (VCF) $\rho(t)$. At low densities or at short times, $\rho(t)$ decays exponentially due to the random uncorrelated collisions between the point particle and the scatterers. At intermediate times $\rho(t)$ drops below $\rho_B(t)$ (the Boltzmann prediction) due to pair correlations. In fact, $\rho(t)$ eventually becomes negative due to backscattering. This represents the RR regime. Finally, at longer times, for all densities, a self-consistent repeated ring (SCRR) theory is required.

At long times,

$$\rho(t) \rightarrow -\alpha' t^{-\beta'} - \alpha t^{-(d+2)/2}$$

where $\beta' > (d+2)/2$. Various theories attempt to describe the long-time behavior of $\rho(t)$.^(4-8,9) All agree that there exists a $t^{-(d+2)/2}$ decay for long times, but disagree on the amplitude α . Several works discuss the preasymptotic $\alpha' t^{-\beta'}$ decay. Gotze, Leutheusser, and Yip (GLY)⁽⁶⁾ and Masters and Keyes (MK)⁽⁴⁾ find that, as ρ_c^* is approached from below, the long-time tail sets in at increasingly longer times. At earlier times, the negative preasymptotic $t^{-\beta'}$ decay dominates. At $\rho^* = \rho_c^*$, the $t^{-\beta'}$ decay persists for all times. While GLY and MK agree on the qualitative behavior of the long-time decay, they disagree on the values of α' , β' , and α .

The molecular dynamics (MD) results of Alder and Alley⁽¹⁰⁾ on the 2D LG show that if $\rho(t)$ is fit to $-\gamma t^{-\delta}$ for times between 15 and 50 mean collision times, then $\delta \approx 2 - 2\rho^*$. It is believed that this reflects an average of the preasymptotic and asymptotic behavior of $\rho(t)$.⁽⁶⁾ The significant MD result is that α is much larger than predicted by any theory.

Using a mode coupling theory, Ernst *et al.* (EMDB)⁽⁸⁾ obtained values for α on the order of one-half the result from MD. However, their theory is not self-contained, requiring rather detailed information concerning the diffusion tensor. This can only be obtained from MD results. The SCRR theory represents an alternative theoretical approach to the determination of α . While MK were able to demonstrate that α becomes very large near

the percolation density, they did not present quantitative predictions on the long-time tail of the VCF.

The purpose of this work is to calculate the VCF over a wide range of times and densities. We utilize an approach similar to that of MK. The approach we follow is discussed in detail in a previous report,⁽¹⁾ hereafter denoted as I [equations from I will be indicated as Eq. (I.1), etc.]. We emphasize that the results presented herein are completely self-contained. We focus primarily on the long-time behavior of $\rho(t)$. In Section 2 we briefly review the approach outlined in I. Section 3 contains results for the two- and three-dimensional Lorentz model. The final section contains a discussion of results and conclusions.

2. OUTLINE OF THE THEORY

We briefly outline the method utilized for the evaluation of the VCF. The method is fully developed in I. Following Masters and Keyes, who applied an integral version of a Cercignani variational principle⁽¹¹⁾ to the solution of the RR equations, a differential variational principle⁽¹²⁾ was presented in I. Equations [Eqs. (I.35)–(I.36)] for the VCF $\rho(t)$ of the tagged particle in the 2D Lorentz model were obtained. They are

$$\begin{aligned} (z + v_B) \rho(z) &= 1 + \langle \mathbf{v}_1 \cdot | T_{12}^{(+)} | \chi^{(2)} \rangle \\ &= 1 + \text{Stat } J(\tilde{\chi}^{(2)}) \end{aligned} \quad (1)$$

where z is the Laplace transform variable, $v_B (= 8v_0\rho^*/3\sigma)$ is the Boltzmann prediction for the friction, and v_0 is the tagged particle's constant speed. $\text{Stat } J(\chi)$ denotes the stationary value of the variational functional $J(\chi)$, where

$$J(\tilde{\chi}^{(2)}) = \langle \tilde{\chi}^{(2)} \cdot | \hat{R} \hat{A}_{\text{LG}} | \tilde{\chi}^{(2)} \rangle - 2 \langle \tilde{\chi}^{(2)} \cdot | \hat{R} \hat{T}_{12}^{(-)} | \chi^{(1)} \rangle \quad (2a)$$

and

$$\hat{A}_{\text{LG}} = z + \mathbf{v}_1 \cdot \frac{\partial}{\partial \mathbf{r}} - \rho \hat{\lambda}(\mathbf{1}, z) - T_{12}^{(-)} \quad (2b)$$

Here \hat{R} is the momentum-space reflection operator and the brackets are defined by

$$\langle f | g \rangle = \frac{1}{2\pi} \int d\mathbf{v}_1 d\mathbf{r}_{12} W_{12}^{(2)} f g \quad (3)$$

where $\mathbf{r}_{12} = \mathbf{r}_1 - \mathbf{r}_2$, and $W_{12}^{(2)}$ is zero for $|\mathbf{r}_1 - \mathbf{r}_2| < \sigma$ and is unity otherwise. The formulas presented here and hereafter are appropriate to the 2D LG,

the formulas in I are appropriate to the 3D LG. In Eq. (2b), the z -dependent, BGK-like approximation to the Lorentz-Boltzmann operator is defined by

$$\rho \hat{\lambda}(\mathbf{1}, z) f(\mathbf{v}_1) = -v(z) \left[f(\mathbf{v}_1) - \frac{1}{4\pi} \int d\hat{v}'_1 f(\mathbf{v}'_1) \right] \quad (4)$$

where $v(z)$ is the z -dependent friction. The motivation for using a z -dependent friction in Eq. (4) lies at the heart of a self-consistent kinetic theory (see Ref. 4 for details). The binary collision operators^(13,14) are defined by

$$T_{jk}^{(\pm)} = \Theta(\pm \dot{l}_{jk}) \delta(l_{jk}) |\dot{l}_{jk}| (\hat{b}_{jk} - 1) \quad (5a)$$

and their adjoints

$$T_{jk}^{(\pm)\dagger} = \delta(l_{jk}) \dot{l}_{jk} \{ \Theta(\pm \dot{l}_{jk}) \hat{b}_{jk} + \Theta(\mp \dot{l}_{jk}) \} \quad (5b)$$

The parameter l_{jk} represents the minimum distance between the surfaces of molecules j and k , \dot{l}_{jk} is the time rate of change of l_{jk} , $\Theta(x)$ and $\delta(x)$ are the Heaviside and delta functions, respectively, and the operator \hat{b}_{jk} acts on the momenta, changing pre- (post-) hit momenta to post- (pre-) hit momenta.

The calculation of $\rho(z)$ proceeds by choosing a variational function $\tilde{\chi}$, which is to mimic the tagged-particle-scatterer pair correlations. In I we argued that a suitable $\tilde{\chi}$ is

$$\tilde{\chi}(\mathbf{r}_{12}, \mathbf{v}, z) = \tilde{\chi}_N(\mathbf{r}_{12}, \mathbf{v}, z) + \tilde{\chi}_K(\mathbf{r}_{12}, \mathbf{v}, z) \quad (6)$$

where χ_K is a completely determined function related to the kinetic boundary layer

$$\chi_K^{(2)} = -(2\rho(z)/v_0^2) \exp\{-[v(z) + z] |\mathbf{r} - \mathbf{r}_0|/v_0\} \hat{r}_0 \cdot \mathbf{v}_1 \hat{r}_0 \Omega(\hat{v}_1) \quad (7a)$$

and χ_N , the normal solution,⁽¹⁵⁾ is given by

$$\tilde{\chi}_N^{(2)} = \left[1 - v(z)^{-1} \mathbf{v}_1 \cdot \frac{\partial}{\partial \mathbf{r}} \right] \tilde{\mathbf{M}}(\mathbf{r}, z) \quad (7b)$$

Here $\tilde{\mathbf{M}}$ is a function of \mathbf{r}_{12} and z to be determined from the variational principle. The kinetic term in Eq. (7a) describes the distribution of particles that have recently undergone a collision at $\mathbf{r}_{12} = \mathbf{r}_0$ with scatterer 2 but have yet to undergo another collision in the fixed fluid. In Eq. (7a), the cone function $\Omega(\hat{v}_1)$ is unity if $-\hat{v}_1$ is directed at the scatterer and is zero otherwise. The normal term $\tilde{\chi}_N$ describes the distant hydrodynamic-like correlations in the tagged-particle-scatterer system.

Inserting Eq. (6a) into the variational function, we obtain

$$\text{Stat } J(\tilde{\mathbf{X}}) = v(z) \rho(z) \{ [\mathbf{M}; \mathbf{S}'] - [\mathbf{S}'; \mathbf{S}'] \} \tag{8}$$

where the square bracket is

$$[\mathbf{A}; \mathbf{B}] = \int d\mathbf{r} W_{12}^{(2)} \mathbf{A}(\mathbf{r}) \cdot \mathbf{B}(\mathbf{r}) \tag{9}$$

$$\mathbf{S}'(\mathbf{r}, z) = -\frac{1}{2\pi} \int d\hat{v} \chi_k^{(2)}(\hat{v}_1, \mathbf{r}, z) \tag{10}$$

and $\mathbf{M}(\mathbf{r}, z)$ is required to be

$$\mathbf{M}(\mathbf{r}, z) = -\frac{v^2(z)}{\pi v_0^2} \int d\mathbf{r}' G(\mathbf{r}, \mathbf{r}' | \omega) \mathbf{S}'(\mathbf{r}', z) \tag{11}$$

Here the Green's function is defined as the solution of the diffusion equation

$$(-\omega^2 + \nabla_r^2) G(\mathbf{r}, \mathbf{r}' | \omega) = -2\pi \delta(\mathbf{r} - \mathbf{r}') \tag{12}$$

where $\omega^2 = 2zv(z)/v_0^2$. Following standard procedures,⁽¹⁶⁾ G is explicitly evaluated as

$$G(\mathbf{r}, \mathbf{r}' | \omega) = \sum_{m=-\infty}^{\infty} \frac{H_{|m|}^{(\ddagger)}(\omega r_>)}{[\delta_{\ddagger,2} - \alpha_{|m|} \delta_{\ddagger,1}]} \times [H_{|m|}^{(1)}(\omega r_<) + \alpha_{|m|} H_{|m|}^{(2)}(\omega r_<)] e^{im(\phi - \phi')} \tag{13}$$

where ϕ and ϕ' are the polar angles of \mathbf{r} and \mathbf{r}' , respectively. Here

$$\ddagger = \begin{cases} 1, & \text{Re } \omega < 0 \\ 2, & \text{Re } \omega > 0 \end{cases} \tag{14}$$

$H_m^{(1)}(x) = I_m(x)$, $H_m^{(2)}(x) = K_m(x)$, I_m and K_m are the modified Bessel functions of the first and second kinds, respectively, $\delta_{n,p}$ represents the Kronecker delta, and

$$\alpha_{|m|} = \frac{H_{|m|-1}^{(1)}(\omega\sigma) + H_{|m|+1}^{(1)}(\omega\sigma)}{H_{|m|-1}^{(2)}(\omega\sigma) + H_{|m|+1}^{(2)}(\omega\sigma)} \tag{15}$$

Thus, from the variational principle, we have determined the unknown

function $\mathbf{M}(\mathbf{r}, z)$. Inserting the explicit form of the Green's function into Eq. (11), we get

$$\mathbf{M}(\mathbf{r}, z) = -\frac{v^2(z)}{v_0^3} \frac{\rho(z)}{\delta_{\ddagger,2} - \alpha_1 \delta_{\ddagger,1}} \times \int_{\sigma}^{\infty} dr' r' H_1^{(\ddagger)}(\omega r_{>}) [H_1^{(\ddagger)}(\omega r_{<}) + \alpha_1 H_1^{(2)}(\omega r_{<})] \mathbf{S}'(r', z) \quad (16)$$

which, with Eqs. (6) and (7), completely specifies χ .

The desired result is obtained by inserting the above forms for $M(r, z)$ into Eq. (8) and utilizing Eq. (1),

$$v_B \rho(z) = \left[z^* + 1 + \frac{v^*(z) \rho^*}{4v_B^*} ([\tilde{s}, \tilde{s}]_{(z)} + v^*(z)^2 [\tilde{n}, \tilde{s}]_{(z)}) \right]^{-1} \quad (17)$$

where the reduced quantities, denoted with a superscript star, are $z^* = z/v_B$, $v^* = v\sigma/v_0$, and $\rho^* = \rho\sigma^2$. The reduced brackets are

$$[\tilde{s}, \tilde{s}]_{(z)} = 2\pi \int_0^1 dy y^{-3} s(y^{-1}, z) s(y^{-1}, z) \quad (18a)$$

$$\begin{aligned} [\tilde{n}, \tilde{s}]_{(z)} = & \frac{4\pi}{\delta_{\ddagger,2} - \alpha_1 \delta_{\ddagger,1}} \left\{ \int_0^1 dy y^{-3} s(y^{-1}, z) \left[H_1^{(1)}\left(\frac{\omega\sigma}{y}\right) \right. \right. \\ & + \alpha_1 H_1^{(2)}\left(\frac{\omega\sigma}{y}\right) \left. \right] \int_0^y dy' y'^{-3} s(y'^{-1}, z) H_1^{(\ddagger)}\left(\frac{\omega\sigma}{y'}\right) \\ & + \int_0^1 dy y^{-3} s(y^{-1}, z) H_1^{(\ddagger)}\left(\frac{\omega\sigma}{y}\right) \int_y^1 dy' y'^{-3} s(y'^{-1}, z) \\ & \times \left[H_1^{(1)}\left(\frac{\omega\sigma}{y'}\right) + \alpha_1 H_1^{(2)}\left(\frac{\omega\sigma}{y'}\right) \right] \left. \right\} \quad (18b) \end{aligned}$$

where

$$s(x, z) = \frac{4}{\pi} \int_0^{\phi_m(x)} d\phi \exp\{-[v^*(z) + v_B^* z^*] d(x, \phi)\} a(x, \phi) b(x, \phi) \quad (19a)$$

$$\phi_m = \arccos[(1 - x^{-2})^{1/2}] \quad (19b)$$

$$a(x, \phi) = [1 - x^{-2}(1 - \mu^2)]^{1/2} = \hat{r}_0 \cdot \hat{v}'_1 \quad (19c)$$

$$b(x, \phi) = a(x, \phi) \mu + \{(1 - \mu^2)[1 - a^2(x, \phi)]\}^{1/2} = \hat{r}_0 \cdot \hat{r} \quad (19d)$$

$$d(x, \phi) = \{[1 - a^2(x, \phi)]/(1 - \mu^2)\}^{1/2} = |\mathbf{r} - \mathbf{r}_0|/R \quad (19e)$$

$$\mu = \cos \phi \quad (19f)$$

This completes the outline of the specific variational solution to the RR VCF. When the parameter $v^*(z)$ in Eqs. (17)–(19) is set equal to v_B^* , we obtain an approximate RR VCF $\rho_{RR}(z)$. However, if we set $\rho(z) = [z + v(z)]^{-1}$, where $v(z)$ is the solution of the implicit equation

$$\frac{v^*(z)}{v_B^*} = 1 + \frac{\rho^* v^*(z)}{\pi v_B^*} [[\tilde{s}, \tilde{s}]_{(z)} + v(z)^2 [\tilde{n}, \tilde{s}]_{(z)}] \quad (20)$$

we obtain a self-consistent form for the VCF $\rho_{SC}(z)$. Equation (20) can be solved by iteration, and the remaining expressions for $\rho_{RR}(z)$ and $\rho_{SC}(z)$ numerically inverse-Laplace-transformed.

3. NUMERICAL RESULTS

3.1. Two-Dimensional Lorentz Gas

We first discuss the numerical results for the two-dimensional Lorentz gas. In Fig. 1 we present the calculation of the diffusion constants, both D_{RR} and D_{SC} , from I and compare with the molecular dynamics of Bruin⁽¹⁷⁾ and Alder and Alley.⁽¹⁰⁾ The diffusion constants are obtained from the $z=0$ friction constants through the relation $D = v_0^2/2v(z=0)$. In I we point out that the choice of trial function is most accurate at high and low

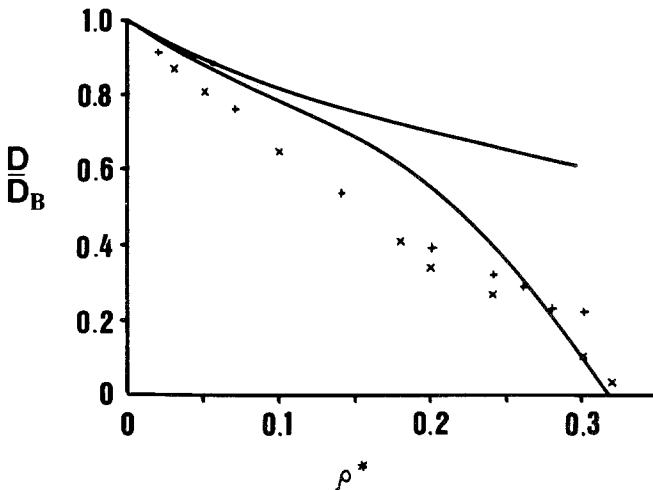


Fig. 1. Density dependence of the diffusion constant in two dimensions. (+) The MD of Bruin, (x) the MD of Alder and Alley; upper curve, the RR calculation; lower curve, the SCRR results.

densities. This observation is reflected in Fig. 1, where the maximum disagreement falls at intermediate densities in the neighborhood of $\rho^* = 0.16$. The difference between D_{RR} and D_{SC} is largely due to a difference in the long-time behavior of $\rho_{RR}(t)$ versus $\rho_{SC}(t)$. We can expect that Fig. 1 will be an indicator of the success of our variational solution in predicting the VCF, in particular the long-time behavior. We should expect the least success at densities around $\rho^* \sim 0.16$ and improved success at higher densities.

Figure 2 presents $\rho_{RR}(t)$ for times from $t=0$ to $t=7.5$ (measured in mean collision times). We observe that as ρ^* is increased, the initial behavior ($t < 3$) of $\rho_{RR}(t)$ changes little, while the amplitudes of the negative portion of $\rho_{RR}(t)$, ($t > 3$), grow. However, the RR approximation underestimates the magnitude of the negative part of $\rho(t)$ and therefore predicts a diffusion constant which is too large. The dashed line in Fig. 2 represents the SC VCF at $\rho^* = 0.24$. Already at seven collision times we observe a difference between the RR and the SCRR approximations. We suspect that this difference results from initial configurations which lead to a large number of tagged-particle-scatterer collisions within the first few mean collision times. Of course, this disagreement $\rho_{RR}(t)$ and $\rho_{SC}(t)$ persists for longer times as well.

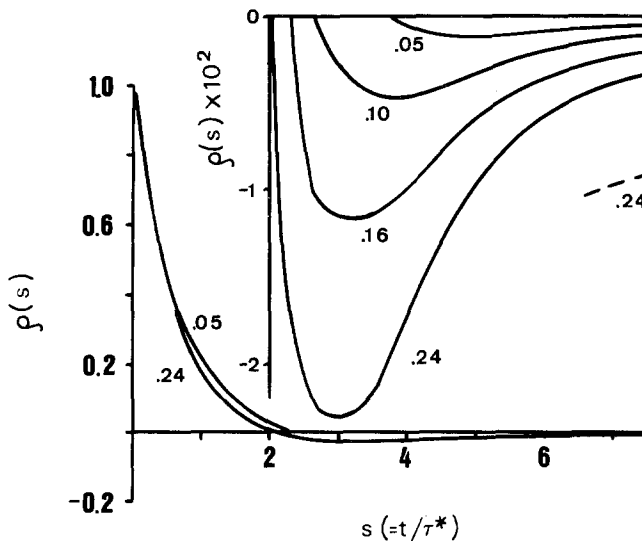


Fig. 2. The RR VCF for four densities. Time is measured in mean collision times. The dashed curve represents the SCRR VCF for $\rho^* = 0.24$. The numbers refer to the reduced density.

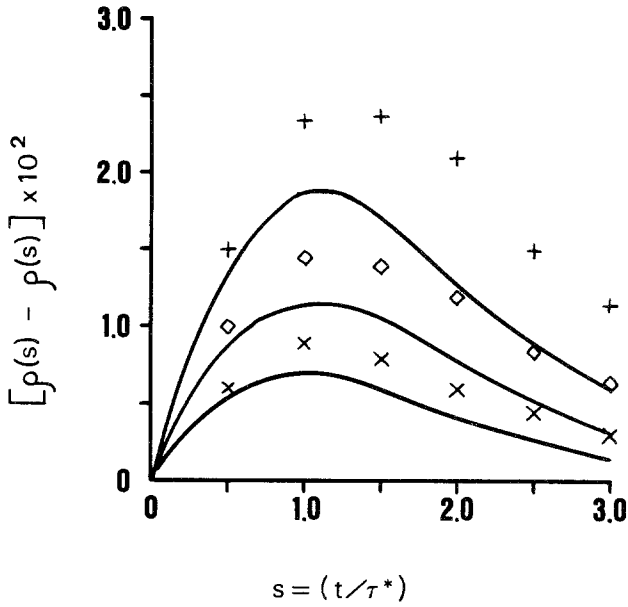


Fig. 3. The deviation of $\rho_{RR}(t)$ from $\rho_B(t)$ ($\times 10^2$) for the 2D LG at three densities, compared with the MD of Bruin. (x) The MD results for $\rho^* = 0.005$, (\diamond) the MD for $\rho^* = 0.01$, (+) MD for $\rho^* = 0.02$.

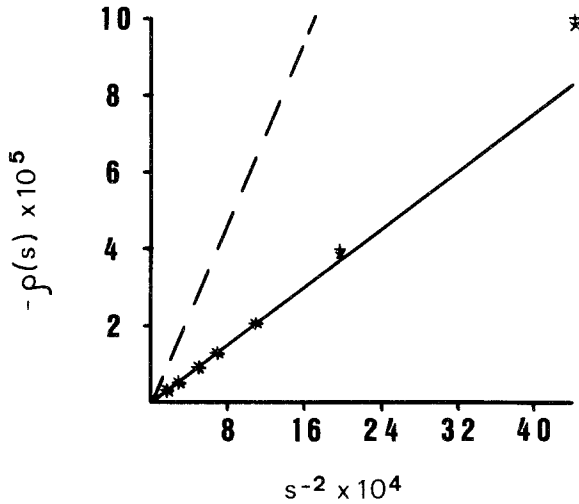


Fig. 4. The long-time behavior of (x) the RR and (+) SCR VCF for the 2D LG at $\rho^* = 0.05$. Also presented are the asymptotic predictions of (- -) MD and (-) RR and SCRR theories.

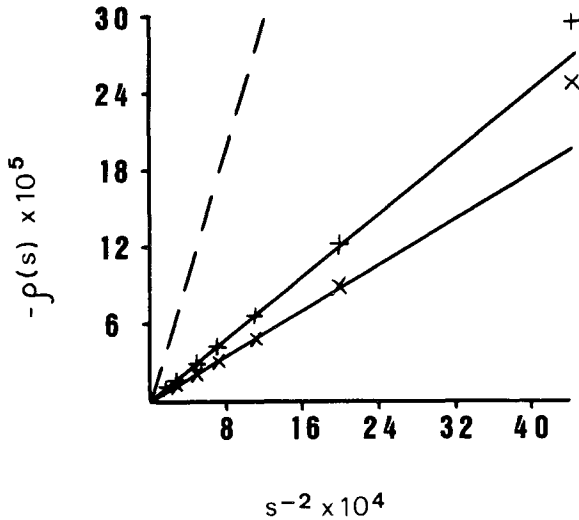


Fig. 5. Similar to Fig. 4, except for $\rho^* = 0.1$.

For times less than approximately three collision times, we expect the RR theory to be sufficient. Figure 3 presents the short-time calculations of the VCF and compares with the MD results of Bruin. The RR theory appears qualitatively correct. At the highest density presented, $\rho^* = 0.02$, the RR theory incorporates approximately 80% of the difference between

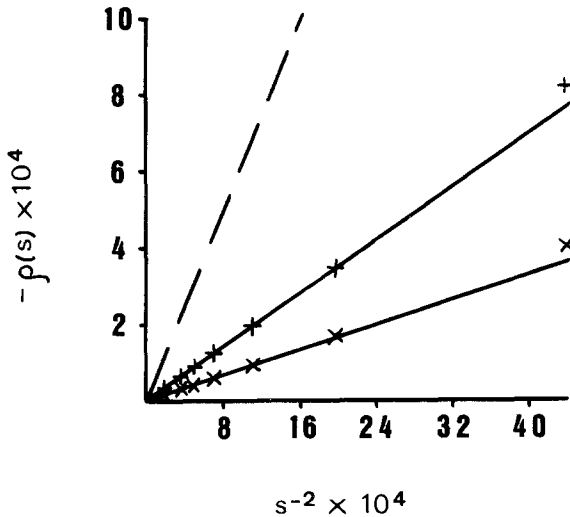


Fig. 6. Similar to Fig. 4, except for $\rho^* = 0.16$.

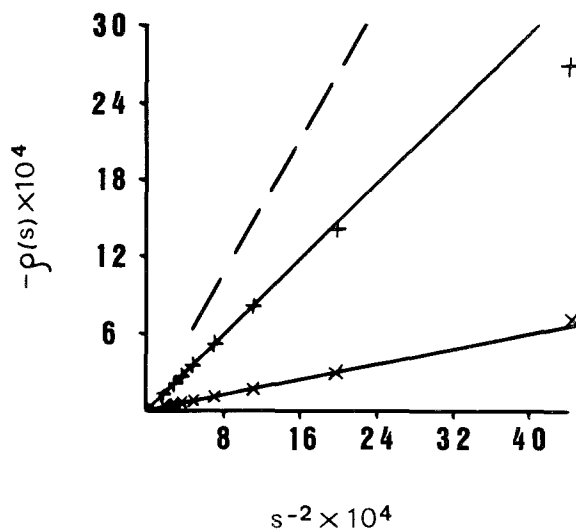


Fig. 7. Similar to Fig. 4, except for $\rho^* = 0.24$.

$\rho(t)$ and $\rho_B(t)$, the Boltzmann prediction. Below we discuss the three-dimensional analogue of Fig. 3 and observe a much improved prediction of the RR theory.

Figures 4–7 present the predicted long-time tails from both RR and SCRR calculations for densities ranging from 0.05 to 0.24. The results are compared with the asymptotic form of $\rho(t)$ from the MD of Alder and Alley. When viewing the long-time tail results, one should keep in mind the error in the density-dependent diffusion constant. We expect the difference between the amplitudes of the tails of the SC and RR calculations to grow with increasing densities. Further, we expect the SC result to improve with increasing densities above $\rho^* \sim 0.16$. These trends are observed in Fig. 4–7. In fact, there exists a dramatic improvement in the prediction for $\rho^* = 0.24$

Table I. Comparison of the Amplitudes of Long-Time Tails for 2D LG Obtained from MD (α_{MD}),⁽¹⁰⁾ Approximate MC (α_{MC}),^(8,9) Repeated Ring (α_{RR}), and Self-Consistent Repeated Ring (α_{SC})

ρ^*	α_{MD}	α_{MC}	α_{RR}	α_{SC}
0.05	0.06	0.03	0.019	0.019
0.10	0.25	0.12	0.042	0.059
0.16	0.62	0.33	0.085	0.169
0.24	1.30	1.33	0.163	0.733

when compared with the $\rho^* = 0.16$ results (where the largest error is expected). It is unfortunate that $\rho^* = 0.24$ is the largest density for which MD results are available.

Table I summarizes the predictions for the amplitudes of the long-time tail. The mode coupling predictions quoted in Table I represent an approximate result obtained from Eq. (4.5) of Ref. 9. The values of α from the SC theory are poor, except for the highest density reported. Here, the SC theory predicts an amplitude within 40% of the MD of Alder and Alley.

3.2. The Three-Dimensional Lorentz Gas

We limit the presentation of the three-dimensional results to the situations studied by Bruin.⁽¹⁷⁾ Figure 8 compares the RR and SCRR values of D with Bruin's MD results. We observe that D_{SC} is in close agreement with the MD over the full density range studied by Bruin. Therefore, we expect the 3D calculations to be more accurate than the 2D calculations of $\rho(t)$. This expectation is substantiated by Figs. 9 and 10, where $\rho_{RR}(t)$ for short times is presented along with MD. The calculations are seen to be extremely accurate not only for $\rho^* = 0.05$, but also for $\rho^* = 0.20$, where the RR theory accounts for 90% of the deviation from $\rho_B(t)$.

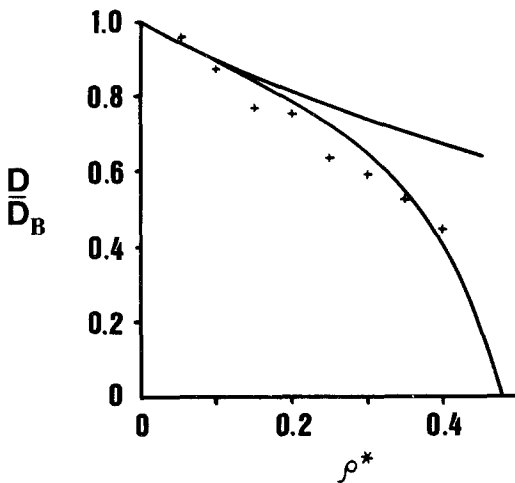


Fig. 8. Density dependence of the diffusion constant for the 3D LG. (+) The MD of Bruin; upper curve, the RR prediction; lower curve, the SCRR prediction.

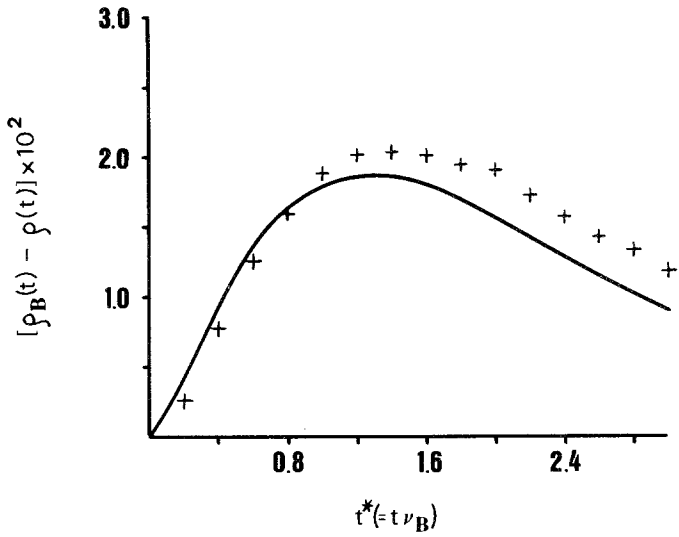


Fig. 9. The deviation of $\rho_{RR}(t)$ from $\rho_B(t)$ ($\times 10^2$) for the 3D LG for $\rho^* = 0.05$. (+) The MD of Bruin.

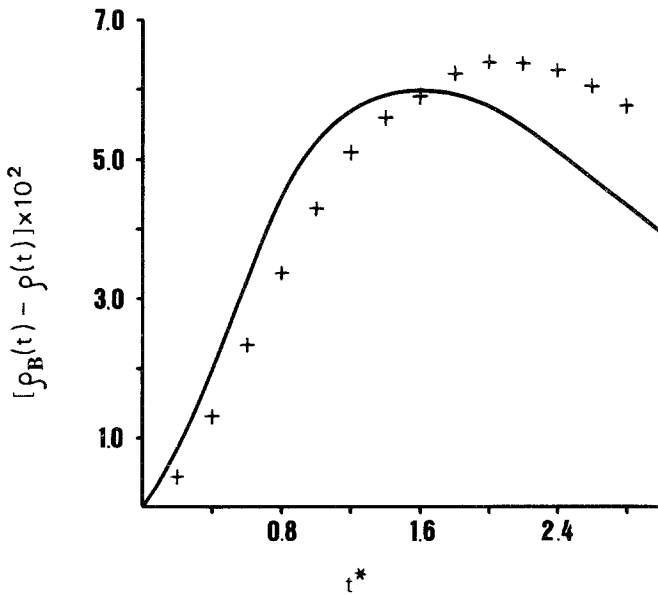


Fig. 10. Similar to Fig. 9, except for $\rho^* = 0.02$.

4. DISCUSSION AND CONCLUSIONS

The trial function utilized in this work was chosen because of its success in reproducing accurate results on the diffusion constant (see Ref. 1) for the Lorentz gas. The diffusion constant calculation utilizing this trial function improved as the density increased. It is apparent that the trial function chosen leads to improved results at high densities for the VCF as well.

It is unfortunate that the 3D MD results are limited, because the 3D LG is simpler to handle theoretically. We believe that the 3D calculations are more accurate than the 2D work and take as evidence Fig. 1 and 3 versus Figs. 8–10. We speculate in I that the superiority of the 3D work rests in the fact that the collision operator is of a BGK form, whereas for the 2D LG this represents an approximation. The BGK assumption (i.e., isotropic scattering cross section) will change not only the nature, but also the extent of the kinetic boundary layer⁽¹⁸⁾ and hence affect χ . Therefore, it would be worthwhile to drop the BGK assumption for the 2D LG and seek an improved solution.

The numerical results here and in I are encouraging and we remain optimistic concerning the approach. The variational method allows for improvement through better trial functions. Furthermore, there is now evidence that a self-consistent kinetic theory set up within the framework of the RR equations represents a suitable approach toward predicting non-equilibrium processes in condensed phases.

ACKNOWLEDGMENTS

We thank the Boston University Computational Center for making their machine available. This work was supported by NSF grant CHE 83-12722.

REFERENCES

1. R. G. Cole and T. Keyes, *J. Stat. Phys.*, this volume, preceding paper.
2. J. R. Dorfman and M. H. Ernst, *Physica* **61**:157 (1972); J. R. Dorfman, in *Fundamental Problems in Statistical Mechanics*, Vol. 3, E. G. D. Cohen, ed. (North-Holland, Amsterdam, 1975).
3. S. W. Haan and R. Zwanzig, *J. Phys. A* **10**:1547 (1977); J. Kertesz, *J. Phys. (Paris)* **42**:L393 (1981).
4. A. Masters and T. Keyes, *Phys. Rev. A* **26**:2129 (1982); **25**:1010 (1982).
5. A. Weijland and J. M. J. van Leeuwen, *Physica* **38**:35 (1968); J. M. J. van Leeuwen, *Physica* **36**:457 (1969); M. H. Ernst and A. Weijland, *Phys. Lett.* **34A**:39 (1971); T. Keyes and J. Mercer, *Physica* **95A**:473 (1979).

6. W. Gotze, E. Leutheusser, and S. Yip, *Phys. Rev. A* **23**:2634 (1981); **24**:1008 (1981); **25**:533 (1982).
7. A. J. Masters, Ph. D. thesis, University of Cambridge (1980), unpublished.
8. M. H. Ernst, J. Machta, J. R. Dorfman, and H. van Beijeren, *J. Stat. Phys.* **34**:477 (1984).
9. J. Machta, M. H. Ernst, H. van Beijeren, and J. R. Dorfman, *J. Stat. Phys.* **35**:413 (1984).
10. B. J. Alder and W. E. Alley, *Physica* **121A**:523 (1983); B. J. Alder and W. E. Alley, *J. Stat. Phys.* **19**:341 (1978); W. E. Alley, Ph.D. thesis, University of California, Davis (1979), unpublished.
11. C. Cercignani, *Theory and Application of the Boltzmann Equation* (Elsevier, New York, 1975).
12. C. Cercignani, *J. Stat. Phys.* **1**:297 (1968).
13. M. H. Ernst, J. R. Dorfman, W. R. Hoegy, and J. M. J. van Leeuwen, *Physica* **45**:127 (1968).
14. R. G. Cole, D. R. Evans, and D. K. Hoffman, *J. Chem. Phys.* **82**:2061 (1985).
15. J. A. McLennan, *Phys. Fluids* **8**:1580 (1965).
16. P. M. Morse and H. Feshbach, *Methods of Theoretical Physics, I and II* (McGraw-Hill, New York, 1953).
17. C. Bruin, *Physica* **72**:261 (1974).
18. R. G. Cole, V. Protopopescu, and T. Keyes, *J. Chem. Phys.* **83**:2384 (1985).